

# Differences in CT Perfusion Maps Generated by Different Commercial Software: Quantitative Analysis by Using Identical Source Data of Acute Stroke Patients<sup>1</sup>

Kohsuke Kudo, MD, PhD  
 Makoto Sasaki, MD, PhD  
 Kei Yamada, MD, PhD  
 Suketaka Momoshima, MD, PhD  
 Hidetsuna Utsunomiya, MD, PhD  
 Hiroki Shirato, MD, PhD  
 Kuniaki Ogasawara, MD, PhD

## Purpose:

To examine the variability in the qualitative and quantitative results of computed tomographic (CT) perfusion imaging generated from identical source data of stroke patients by using commercially available software programs provided by various CT manufacturers.

## Materials and Methods:

Institutional review board approval and informed consent were obtained. CT perfusion imaging data of 10 stroke patients were postprocessed by using five commercial software packages, each of which had a different algorithm: singular-value decomposition (SVD), maximum slope (MS), inverse filter (IF), box modulation transfer function (bMTF), and by using custom-made original software with standard (sSVD) and block-circulant (bSVD) SVD methods. Areas showing abnormalities in cerebral blood flow (CBF), mean transit time (MTT), and cerebral blood volume (CBV) were compared with each other and with the final infarct areas. Differences among the ratios of quantitative values in the final infarct areas and those in the unaffected side were also examined.

## Results:

The areas with CBF or MTT abnormalities and the ratios of these values significantly varied among software, while those of CBV were stable. The areas with CBF or MTT abnormalities analyzed by using SVD or bMTF corresponded to those obtained with delay-sensitive sSVD, but overestimated the final infarct area. The values obtained from software by using MS or IF corresponded well with those obtained from the delay-insensitive bSVD and the final infarct area. Given the similarities between CBF and MTT, all software were separated in two groups (ie, sSVD and bSVD). The ratios of CBF or MTTs correlated well within both groups, but not across them.

## Conclusion:

CT perfusion imaging maps were significantly different among commercial software even when using identical source data, presumably because of differences in tracer-delay sensitivity.

© RSNA, 2010

Supplemental Material: <http://radiology.rsna.org/lookup/suppl/doi/10.1148/radiol.254082000/-/DC1>

<sup>1</sup> From the Advanced Medical Research Center (K.K. and M.S.), Department of Neurosurgery (K.O.), Iwate Medical University; 19-1 Uchimaru, Morioka 020-8505, Japan, Department of Radiology, Kyoto Prefectural University of Medicine, Kyoto, Japan (K.Y.); Department of Radiology, Keio University, Tokyo, Japan (S.M.); Department of Radiology, Fukuoka University School of Medicine, Fukuoka, Japan (H.U.); Department of Radiology, Hokkaido University Graduate School of Medicine, Sapporo, Japan (H.S.). Received November 12, 2008; revision requested February 4, 2009; revision received May 7; accepted June 2; final version accepted June 17. Supported in part by the Research Grant for Cardiovascular Diseases (17C-3) from the Ministry of Health, Labour and Welfare of Japan, and by a Grant-in-Aid for Advanced Medical Science Research from the Ministry of Education, Culture, Sports, Science and Technology of Japan. **Address correspondence to K.K.** (e-mail: [kokudo@iwate-med.ac.jp](mailto:kokudo@iwate-med.ac.jp)).

Computed tomographic (CT) perfusion imaging is a widely applied technique for initial evaluation of acute ischemic stroke patients, including prediction of tissue at risk and patient outcome (1–3); it is also used to assess other diseases such as hemodynamic ischemia (4), subarachnoid hemorrhage (5), and brain tumors (6). Commercial software packages for CT perfusion analysis are now available with CT systems from all manufacturers and facilitate the use of CT perfusion imaging. Although one of the advantages of CT perfusion imaging is its quantitative nature, it has been reported that the results of CT perfusion imaging analysis vary substantially owing to differences in scan parameters, such as tube voltage (7,8), tube current (8), and temporal resolution (9). Variations have also been reported in postprocessing steps, such as the definition of arterial input function and venous output function (10), determination of bolus timing (11), and deconvolution algorithms (12,13). However, previous studies have not focused on the differences among commercial software that use different algorithms. The differences among software can be important when interpreting perfusion abnormalities, comparing results among studies, and adopting CT perfusion imaging as a criterion for patient selection in multicenter trials.

The purpose of our study was to examine the variability in the qualitative and quantitative results of CT perfusion imaging generated from identical

source data of stroke patients by using commercially available programs provided by various CT manufacturers.

## Materials and Methods

### Subjects

Our study protocol was approved by the institutional review board; written informed consent was obtained from the family members of all patients. Ten consecutive patients with acute ischemic stroke caused by major arterial occlusion (seven men, three women) were retrospectively collected (Table E1 [online]). All patients also underwent unenhanced CT imaging, CT perfusion imaging, and CT angiography at admission and during follow-up. One patient had extracranial carotid occlusion (case 2) and six (cases 1, 3, 4, 5, 8, and 9) were diagnosed as intracranial embolic occlusion owing to arterial fibrillation. The etiologic outcome of the other three patients was not determined. Thrombolytic therapy was performed in one patient (case 1) and the other nine were treated conservatively. No recanalization was seen at follow-up CT angiography.

### CT Examination

After performing unenhanced CT with a four detector-row scanner (Aquilion; Toshiba Medical Systems, Tokyo, Japan), CT perfusion imaging was performed with an intravenous bolus injection of contrast agent (40 mL of iopamidol; Bayer HealthCare, Berlin, Germany) injected at a rate of 5 mL/sec. Four sections, including the basal ganglia, were imaged simultaneously without table movement and by using the fol-

lowing scan parameters: field of view, 240 mm; section thickness, 8 mm; gantry rotation speed, 1.0 sec; tube voltage, 120 kVp; and tube current, 70 mA. The total scan time was 50 sec. After CT perfusion imaging, intracranial CT angiography was performed by using 60 mL of the same contrast agent.

### Postprocessing of CT Perfusion Imaging Data

After anonymization, the CT perfusion imaging data were postprocessed by one author (K.K., with 8 years experience in stroke imaging) by using five commercial software packages for CT perfusion imaging analysis developed by five manufacturers (Table 1) without access to any patient information except that of the affected sides. The maximum slope (MS) method was used in software D (1). The deconvolution method was used in the other four packages, which utilized various algorithms, such as singular-value decomposition (SVD): software A (14) and C (9), in

## Advances in Knowledge

- There were significant differences in the abnormal areas and quantitative values of cerebral blood flow (CBF) and mean transit time (MTT) among five commercial software packages provided by CT manufacturers; conversely, values for cerebral blood volume were almost identical among all five.
- All software used can be divided in two groups according to the tracer-delay sensitivity for CBF and MTT measurements.

## Implications for Patient Care

- Overestimation of abnormalities in CBF and MTT values, presumably owing to the tracer-delay effect, occurred in software utilizing delay-sensitive algorithms.
- Estimation of the final infarct region size can be more reliably determined by using CBF and MTT with delay-insensitive software than with delay-sensitive software.

### Published online

10.1148/radiol.254082000

**Radiology 2010**; 254:200–209

### Abbreviations

bMTF = box modular transfer function  
 bSVD = block-circulant SVD  
 CBF = cerebral blood flow  
 CBV = cerebral blood volume  
 IF = inverse filter  
 MS = maximum slope  
 MTT = mean transit time  
 PMA = Perfusion Mismatch Analyzer  
 rCBF = relative CBF  
 rCBV = relative CBV  
 rMTT = relative MTT  
 ROI = region of interest  
 sSVD = standard SVD  
 SVD = singular-value decomposition  
 TTP = time to peak

### Author contributions:

Guarantors of integrity of entire study, K.K., M.S.; study concepts/study design or data acquisition or data analysis/interpretation, all authors; manuscript drafting or manuscript revision for important intellectual content, all authors; approval of final version of submitted manuscript, all authors; literature research, M.S., K.Y.; clinical studies, K.K., H.U.; statistical analysis, K.K., M.M.; and manuscript editing, K.K., M.S., K.Y., M.M., H.S., K.O.

Authors stated no financial relationship to disclose.

Table 1

List of Software			
Software	Manufacturer	Version	Analysis Algorithm
A	GE Healthcare	CT Perfusion 3	SVD
B	Hitachi Medical Systems	2.0	IF
C	Philips Medical Systems	1.201	SVD
D	Siemens Medical Systems	VA70A	MS
E	Toshiba Medical Systems	Ph 7	bMTF

which the details of the SVD algorithm have not been disclosed; an inverse filter (IF) method with software B (15); and a box-modulated transfer function (bMTF) with software E (16). The same CT perfusion imaging data were also analyzed by using a free software program, Perfusion Mismatch Analyzer (PMA) (17) to obtain results that served as a reference. PMA was developed as standardized software in the activity of Acute Stroke Imaging Standardization group in Japan (18). Two deconvolution algorithms, standard SVD (sSVD) (19) and block-circulant SVD (bSVD) (20), were used with PMA, as the characteristics of these algorithms are well documented, particularly in terms of sensitivity to the tracer-delay effect (13,20,21). In addition, PMA uses the same core algorithm of SVD as used in the previous report (22), the quantitative values of which were validated with positron emission tomography (PET). In both types of SVD algorithms, a fixed threshold level of 0.2 was used as the cutoff value for diagonal matrices.

The positions of arterial input function and venous output function were manually set at the insular segment (M2) of the middle cerebral artery on the unaffected side and at the posterior part of the superior sagittal sinus, respectively. Positioning was performed carefully to ensure consistency among all software. Quantitative maps of cerebral blood flow (CBF), cerebral blood volume (CBV), and mean transit time (MTT) were generated. For software D, time-to-peak (TTP) maps were generated instead of MTT maps.

#### Data Analysis

CBF, CBV, and MTT/TTP maps generated by using all software, maps gen-

erated with sSVD and bSVD, and the follow-up unenhanced CT images were loaded in PMA and coregistered. All perfusion maps were displayed by using the identical color lookup table. The range of the color scale was determined automatically, as described in a previous report (ie, the top value was set to twice the average value of the unaffected hemisphere, the bottom value was set to zero) (12). Vascular pixel elimination was applied by using a previously described method (22), in which the threshold for a vascular pixel was 1.5 times the average CBV of the unaffected hemisphere.

After randomization of the maps, a polygonal region of interest (ROI) was manually drawn on the visually abnormal areas of the perfusion maps by an author (M.S., with 20 years experience in stroke imaging) who was unaware of the patients' information. The areas of the final infarct defined as hypodense at follow-up CT were measured by using the same manual ROI tracing technique. These ROIs were obtained three times at 2-week intervals and their areas were averaged for further analysis.

CBF, CBV, and MTTs of the final infarct area were measured by superimposing the ROI of the final infarct area over each perfusion map. The relative values of CBF, CBV, and MTT (rCBF, rCBV, and rMTT, respectively; ie, ratios of the values obtained from the affected side to the values obtained from the corresponding contralateral unaffected side), were calculated by using an ROI mirrored to the midline of the cerebral hemispheres.

#### Statistical Analysis

A one-way repeated-measures analysis of variance on ranks (the Friedman test)

was used to determine whether there was a significant difference between the areas of final infarct and abnormal CBF, CBV, and MTT ROIs. Analysis performed with each software represented repeated-measures analysis. If there was a significant difference, the post hoc Dunnett test was used to determine which software had produced a significantly different area compared with the final infarct (control). Differences in rCBF, rCBV, and rMTTs in the final infarct area among different software were also examined by using the same method, in which the values obtained with sSVD or bSVD of the PMA program were used as controls. TTP maps generated with software D were excluded from the analysis of these relative value comparisons.

Correlations between abnormal areas and relative values in the final infarcts between each pair of software were evaluated by using the Spearman correlation coefficient and linear regression. Intraoperator agreement in the repeated ROI measurements was examined by using an intraclass correlation coefficient. An  $\alpha$  level of .05 was used for all statistical tests to indicate significance.

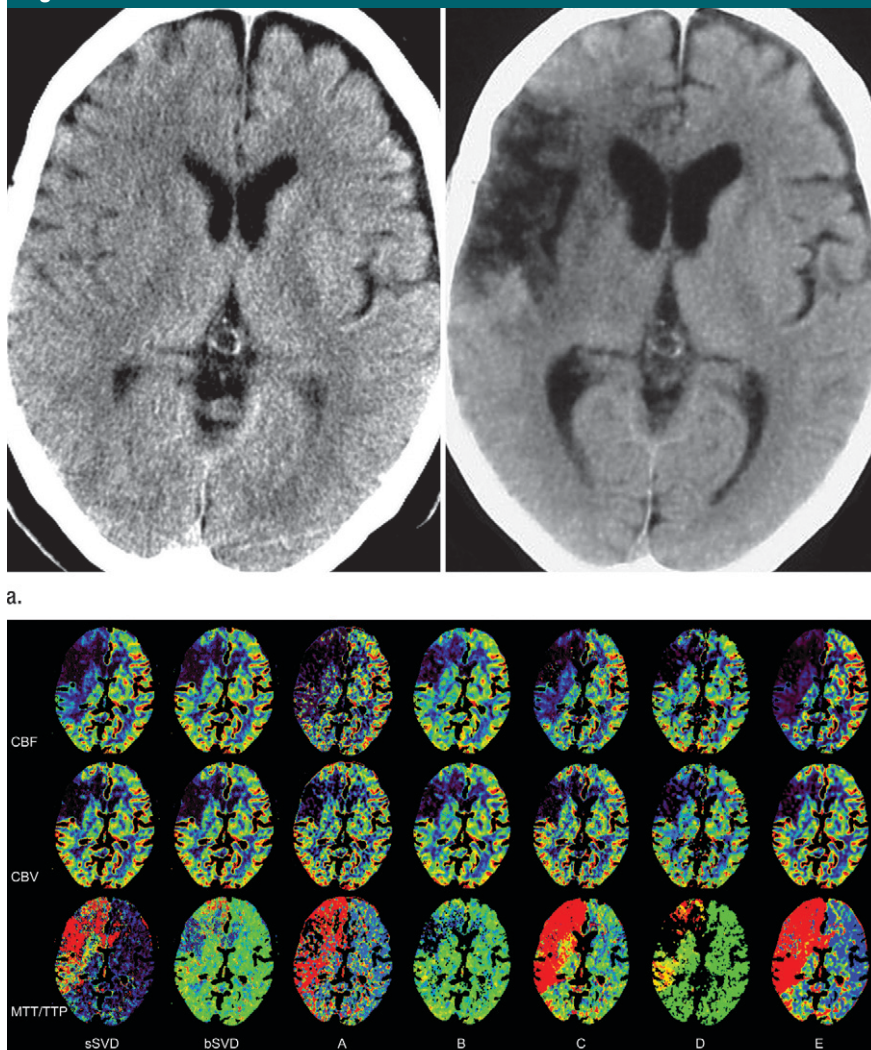
## Results

### Areas of Perfusion Abnormalities

There were significant differences in the areas with CBF, MTT/TTP, or CBV abnormalities among all software packages, two SVD techniques in PMA, and the final infarct size (one-way repeated-measures analysis of variance on ranks;  $P < .0001$  for all).

Images that showed a decrease in CBF measured by using SVD (software A, C) and bMTF (software E) methods correlated well with those measured by using sSVD methods with PMA and were significantly larger than the final infarct size. However, the abnormal areas measured by using IF (software B) and MS (software D) methods correlated with those measured by using bSVD methods as well as the final infarct size (Figs 1, 2a). There were significant correlations between each pair of images among SVD, bMTF, and sSVD methods

Figure 1



a.

**Figure 1:** Perfusion maps generated from identical source data by using different software. **(a)** Unenhanced CT images and **(b)** perfusion maps in 73-year-old man with right middle cerebral artery occlusion (case 9). CBF, CBV, and MTT/TTP maps generated with all software and by using sSVD and bSVD methods are displayed with same color lookup table, automatic color scale determination, and vascular pixel elimination. On unenhanced scan at admission (**a**, left), faint hypodense areas in right frontal operculum and basal ganglia are noted and final infarct area is identified on follow-up unenhanced scan (**a**, right). Decrease in CBF area measured with sSVD is much larger than that measured with bSVD, which is comparable with final infarct area. Software A, C, and E show almost same CBF changes as sSVD, while software B and D show almost same changes as bSVD. Abnormal MTT/TTP areas in sSVD and software A, C, D, and E were apparently larger than those in bSVD, software B, and final infarct area. Note that erroneous MTT/TTP decrease in software A, B, D, and bSVD is seen in area of significant CBV decrease. Areas with CBV decrease are almost same among all software.

and between each pair of images among IF, MS, bMTF, and bSVD methods. We found only weak correlations between the pairs among the two aforementioned groups (sSVD and bSVD, Table 2).

Areas with MTT/TTP abnormalities also varied markedly among software (Figs 1, 2b). Abnormal TTP and MTT areas measured by using SVD, bMTF, and sSVD were significantly larger than

the final infarct size and showed significant correlations between each pair among these (Fig 2b, Table 2). In contrast, the areas with MTT abnormalities measured by using IF and bSVD had a significant correlation, and corresponded well with the final infarct size (Fig 2b, Table 2).

Areas with decrease in CBV, which were significantly smaller than the final infarct size, were not different among the software, and correlated well with each other (Figs 1 and 2c, and Table 2).

### Relative Values in Final Infarct Area

Differences among rCBF, rMTTs, and rCBV in the final infarct area were significant among software (one-way repeated-measures analysis of variance on ranks;  $P < .0001$  for all values).

rCBF measured with SVD (software A and C), MS (software D), and bMTF (software E) were significantly smaller than those measured with bSVD but were not different from those measured with sSVD. While rCBF measured with IF (software B) were significantly larger than those measured with sSVD, they were not different from those measured with bSVD (Fig 3a). There were significant correlations between almost each pair of software, particularly between those utilizing IF, MS, sSVD, and bSVD (Table 3).

rMTTs in the final infarct areas varied remarkably among software (Fig 3b). rMTTs measured with SVD and bMTF were significantly larger than those measured with bSVD and sSVD. Moreover, the values measured with IF were significantly lower than those measured with sSVD, but not those measured with bSVD (Fig 3b). However, significant correlations were observed among software, except for bMTF, particularly between IF and bSVD (Table 3).

rCBVs were nearly constant (Fig 3c) when compared with the variations in rCBF and rMTT values. There were significant correlations between almost all the combinations of these software (Table 3).

### Intraoperator Agreements

Intraoperator agreements (intraclass correlation coefficients) in the three

Figure 2

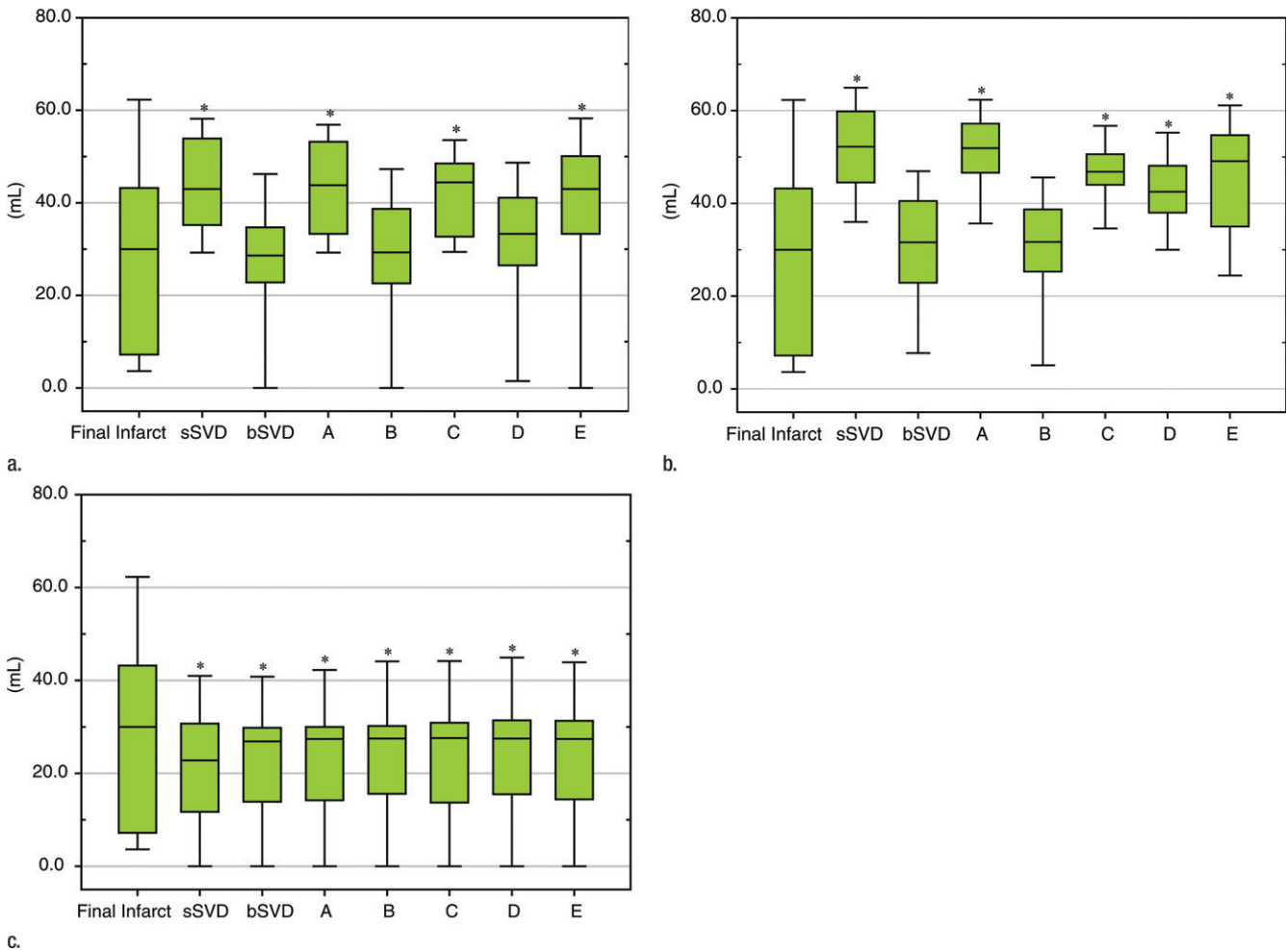


**Figure 2:** Differences in areas with perfusion abnormalities among various software. Areas of final infarct and those of perfusion abnormalities in (a) CBF, (b) MTT/TTP, and (c) CBV measured with sSVD and bSVD and with all software are shown. Sizes of abnormal CBF or MTT/TTP areas vary significantly among software. Areas with CBF abnormalities measured with software A, C, and E are similar to those measured with sSVD and are significantly larger than final infarct size. Areas measured with software B and D and with bSVD are comparable with each other and are not significantly different from final infarct size. Areas with MTT abnormalities measured with software A, C, and E and with sSVD and those with TTP abnormalities measured with software D are significantly larger than final infarct size; those measured with software B and bSVD were not significantly different from final infarct. In contrast, areas with CBV abnormalities are nearly equal among software and are significantly smaller than final infarct size. \* = Significant ( $P < .05$ ) difference compared with final infarct size, derived by using post hoc Dunnett test of one-way repeated-measures analysis of variance.

repeated ROIs for areas of abnormalities in the CBF, CBV, and MTT/TTP maps, as well as the final infarct areas, were 0.997, 0.991, 0.994, and 0.978, respectively.

## Discussion

In this study, perfusion maps were successfully generated by using commercially available software packages from five CT manufacturers under nearly identical analysis conditions but with

different algorithms. Although the manufacturers do not always provide end-users with precise information concerning their postprocessing techniques, we could compare the results of these programs with each other, with those derived by using the common algorithms such as sSVD and bSVD, and with the final infarct size.

The areas with CBF or MTT/TTP abnormalities substantially varied among the software. However, the areas with

CBF decrease or MTT increase measured with SVD and bMTF algorithms were similar to those measured with sSVD and corresponded well with each other, while those measured with IF and MS were similar to those measured with bSVD with excellent correlation. Hence, the software appear to be divided in two groups: those that appear equivalent to sSVD (group 1; software A, C, and E), and those that appear equivalent to bSVD (group 2; software

**Table 2**

**Areas of Perfusion Abnormality Measured between Software Programs**

Linear Regression	Spearman Correlation Coefficient						
	sSVD	bSVD	Software A	Software B	Software C	Software D	Software E
<b>CBF abnormality</b>							
sSVD	...	0.316*	0.959*	0.367*	0.821*	0.512*	0.829†
bSVD	y = 0.262x + 36.485	...	0.284†	0.964*	0.280*	0.882*	0.515†
Software A	y = 0.997x + 0.252	y = 0.467x + 6.430	...	0.324*	0.825*	0.480*	0.791†
Software B	y = 0.255x + 36.445	y = 0.946x + 0.588	y = 0.216x + 37.368	...	0.317*	0.916*	0.551†
Software C	y = 0.898x + 5.05	y = 0.341x + 13.473	y = 0.871x + 6.077	y = 0.482x + 6.962	...	0.377*	0.748†
Software D	y = 0.299x + 34.321	y = 0.890x - 0.603	y = 0.258x + 35.414	y = 0.935x - 1.066	y = 0.192x + 36.885	...	0.621
Software E	y = 0.385x + 28.578	y = 0.584x + 4.122	y = 0.354x + 29.651	y = 0.604x + 4.224	y = 0.283x + 31.825	y = 0.664x + 4.970	...
<b>MTT/TTP abnormality</b>							
sSVD	...	0.514*	0.843*	0.431*	0.773*	0.653*	0.744†
bSVD	y = 0.315x + 42.333	...	0.357*	0.863*	0.280†	0.230†	0.259†
Software A	y = 1.027x - 0.830	y = 0.322x + 12.893	...	0.243†	0.862*	0.792*	0.687*
Software B	y = 0.216x + 45.367	y = 0.878x + 4.034	y = 0.065x + 49.133	...	0.176	0.152	0.186
Software C	y = 1.215x - 4.965	y = 0.341x + 13.473	y = 13117x - 1.019	y = 0.174x + 20.758	...	0.875*	0.632*
Software D	y = 0.808x + 16.872	y = 0.274x + 17.550	y = 0.757x + 18.454	y = 0.144x + 22.670	y = 0.692x + 16.834	...	0.617*
Software E	y = 0.585x + 24.915	y = 0.173x + 21.439	y = 0.454x 30.321	y = 0.039x + 27.067	y = 0.354x + 30.455	y = 0.460x + 22.054	...
<b>CBV abnormality</b>							
sSVD	...	0.977*	0.967*	0.972*	0.954*	0.962*	0.961*
bSVD	y = 0.987x - 0.075	...	0.987*	0.981*	0.966*	0.977*	0.973*
Software A	y = 0.961x + 0.496	y = 0.974x + 0.581	...	0.974*	0.961*	0.967*	0.968*
Software B	y = 0.944x + 0.314	y = 0.954x + 0.452	y = 0.977x - 0.08	...	0.957*	0.971*	0.962*
Software C	y = 0.947x + 0.534	y = 0.958x + 0.655	y = 0.980x + 0.16	y = 1.001x + 0.297	...	0.970*	0.989*
Software D	y = 0.944x - 0.214	y = 0.955x - 0.109	y = 0.976x - 0.602	y = 0.998x - 0.514	y = 0.993x - 0.702	...	0.984*
Software E	y = 0.945x + 0.321	y = 0.957x + 0.421	y = 0.98x - 0.098	y = 1.0x + 0.057	y = 0.991x - 0.054	y = 0.992x + 0.787	...

\* P < .01.

† P < .05.

B and D). These results suggest that CBF and MTT maps can provide similar information concerning perfusion abnormalities when the software belong to the same group, but not when in different groups.

It is well known that the difference between the sSVD and bSVD algorithms is in the tracer-delay sensitivity. In fact, bSVD was developed as a delay-insensitive technique on the basis of the delay-sensitive sSVD algorithm (20). While sSVD may produce erroneous CBF decrease and MTT increase in areas where tracer arrival is simply delayed without any changes in CBF/MTT, bSVD yields stable CBF and MTT values even with tracer delay (13). In our study, the areas with CBF abnormalities in group 1 (software A, C, and E) were significantly larger than those in group 2 (software B and D). This

result suggests that SVD algorithms used in software A and C are presumably sSVD or its equivalents, and that bMTF is sensitive to tracer delay. This result also supports the belief that the IF method (15), a mathematic equivalent of fast-Fourier transform (19), and the MS method (1) (an estimation of CBF by using the maximum slope of the time-density curve) are independent of tracer delay. TTP is known to be dependent on the tracer delay, and should therefore be included in group 1.

Prediction of the irreversible infarct core is an important factor in identifying the tissue at risk by using a mismatch concept and in strategies for management of acute stroke. Previous reports demonstrated that abnormal CBF decrease correlated well with the final infarct in the case of the delay-insensitive MS method by using CT per-

fusion imaging (2) and delay-corrected SVD by using magnetic resonance (MR) perfusion (23), while the final infarct size was overestimated by using SVD with CT perfusion imaging (24) and MR perfusion imaging (23,25). In our study, none of the patients showed recanalization of occluded vessels. Abnormal CBF/MTT areas in the delay-sensitive software lead to overestimation of the final infarct size, while CBF/MTT areas in the delay-insensitive software corresponded well. Therefore, delay-insensitive algorithms are preferable for estimating the final infarct size.

Evaluation of ischemic severity is another important factor in assessing acute ischemic stroke. In general, semi-quantitative values, such as the ratio to the contralateral unaffected hemisphere, are considered as more reliable than the absolute values because the former

Figure 3

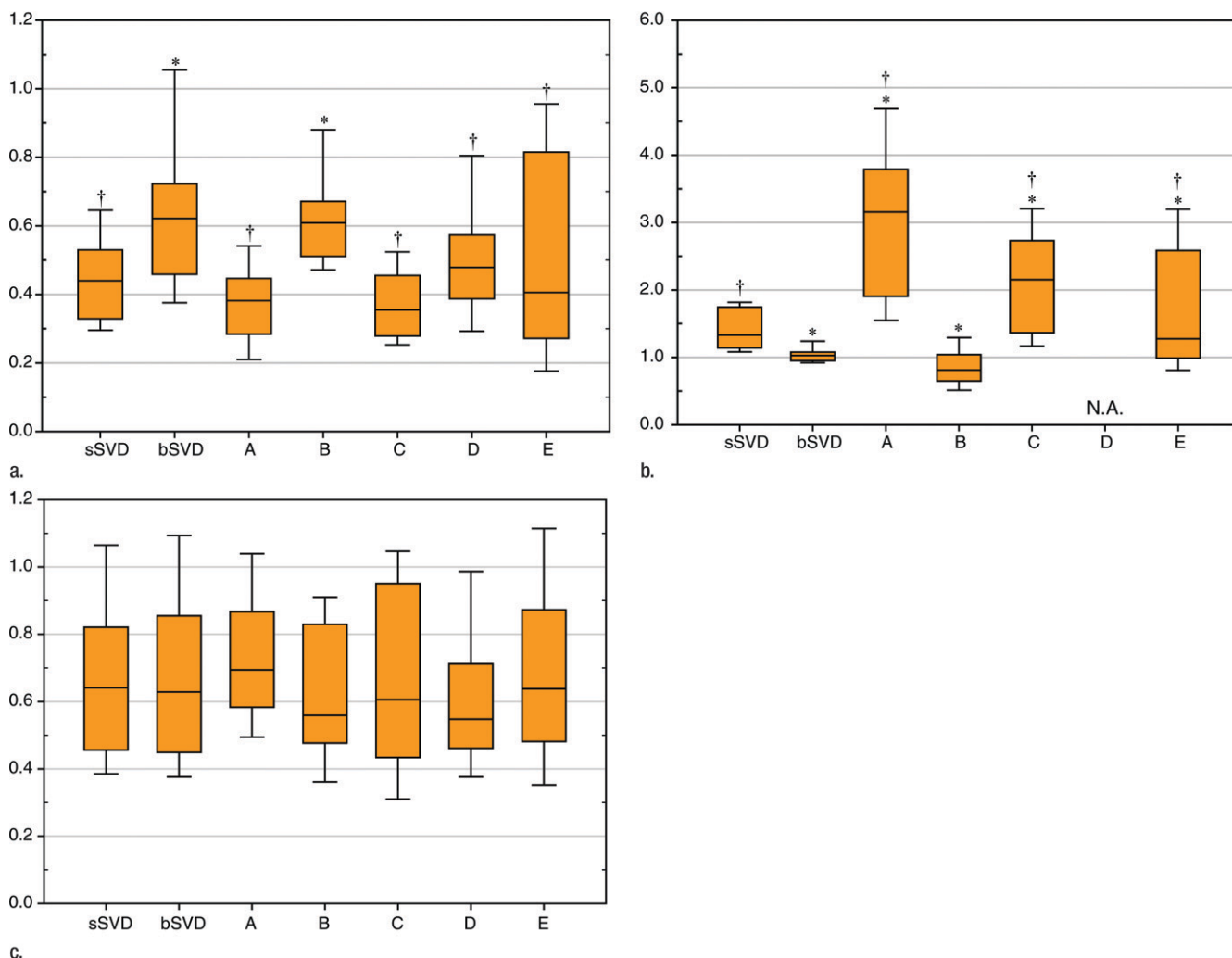


**Figure 3:** Difference in relative ratios of perfusion parameters among various software. **(a)** rCBF, **(b)** rMTT, and **(c)** rCBV in final infarct areas to contralateral unaffected side were analyzed by using sSVD, bSVD, and all software are shown. rCBF values obtained with software B are significantly greater than those obtained with sSVD but are not significantly different to those obtained with bSVD, while those obtained with software A, C, D, and E are significantly smaller than those obtained with bSVD. rMTTs vary remarkably among software; those obtained with software A, C, and E are significantly larger than those obtained with bSVD, while those obtained with software A, B, and C are significantly different from those obtained with sSVD. Variations of rCBVs are smaller among software. \* = Significantly ( $P < .05$ ) different from sSVD, † = significantly ( $P < .05$ ) different from bSVD; by post hoc Dunnett test of one-way repeated-measures analysis of variance.

can eliminate variations in absolute values among software. For this reason, we evaluated the relative ratios instead of the absolute values. However, we found that substantial intervendor differences in rCBF and rMTTs still existed.

rCBF and rMTTs are dependent on the susceptibility of the algorithms to tracer delay. The superiority of delay-insensitive algorithms such as bSVD has been demonstrated in chronic ischemia in both CT perfusion imaging

(12) and MR perfusion imaging (26), in which bSVD showed better correlation with single-photon emission tomography (SPECT) than sSVD. In our study, rCBF values of the final infarct areas in the delay-sensitive software were significantly smaller than in the delay-insensitive software, supporting previous reports. We also found that delay-insensitive MS underestimated

rCBF and delay-sensitive SVD methods showed larger rMTTs than sSVD. Hence, rCBF and rMTTs can be affected not only by the tracer-delay effect but also by other factors during postprocessing, such as the denoising filter, curve fitting, and regularization of deconvolution. For example, a number of zero-MTT pixels were seen in some software, which was presumably a result of inaccurate calculation in severely hypoperfused tissue.

**Table 3**

**Relative Ratios Measured between Software**

Linear Regression	Spearman Correlation Coefficient						
	sSVD	bSVD	Software A	Software B	Software C	Software D	Software E
<b>CBF</b>							
sSVD	...	0.935*	0.912*	0.953*	0.812*	0.899*	0.462*
bSVD	$y = 0.556x + 0.098$	...	0.782*	0.949*	0.780*	0.966*	0.325*
Software A	$y = 1.039x + 0.054$	$y = 1.438x + 0.082$	...	0.819*	0.777*	0.781*	0.409*
Software B	$y = 0.792x - 0.045$	$y = 1.332x - 0.200$	$y = 0.513x + 0.069$	...	0.791*	0.927*	0.382*
Software C	$y = 1.077x + 0.044$	$y = 1.534x + 0.054$	$y = 0.882x + 0.049$	$y = 1.147x + 0.192$	...	0.734*	0.354*
Software D	$y = 0.690x + 0.109$	$y = 1.229x + 0.025$	$y = 0.461x + 0.153$	$y = 0.856x + 0.202$	$y = 0.335x + 0.209$	...	0.228 <sup>†</sup>
Software E	$y = 0.240x + 0.325$	$y = 0.403x + 0.422$	$y = 0.174x + 0.290$	$y = 0.296x + 0.471$	$y = 0.119x + 0.316$	$y = 0.277x + 0.349$	...
<b>MTT</b>							
sSVD	...	0.749*	0.695*	0.834*	0.588*	Not applicable	0.375*
bSVD	$y = 1.961x - 0.620$	...	0.756*	0.923*	0.733*	Not applicable	0.627*
Software A	$y = 0.18x + 0.887$	$y = 0.06x + 0.862$	...	0.718*	0.654*	Not applicable	0.564*
Software B	$y = 0.941x + 0.613$	$y = 0.383x + 0.711$	$y = 2.739x + 0.627$	...	0.775*	Not applicable	0.598*
Software C	$y = 0.092x + 1.213$	$y = 0.061x + 0.901$	$y = 0.435x + 1.992$	$y = 0.14x + 0.542$	...	Not applicable	0.761*
Software D	Not applicable	Not applicable	Not applicable	Not applicable	Not applicable	...	Not applicable
Software E	$y = 0.063x + 1.309$	$y = 0.05x + 0.95$	$y = 0.37x + 2.311$	$y = 0.104x + 0.672$	$y = 0.596x + 1.198$	Not applicable	...
<b>CBV</b>							
sSVD	...	0.986*	0.963*	0.937*	0.922*	0.959*	0.953*
bSVD	$y = .0968x + 0.014$	...	0.965*	0.952*	0.934*	0.962*	0.976*
Software A	$y = 1.096x - 0.148$	$y = 1.127x + 0.164$	...	0.916*	0.889*	0.931*	0.935*
Software B	$y = 1.131x - 0.051$	$y = 1.177x - 0.072$	$y = 0.984x + 0.119$	...	0.899*	0.968*	0.947*
Software C	$y = 0.784x + 0.134$	$y = 0.813x + 0.122$	$y = 0.665x + 0.291$	$y = 0.676x + 0.175$	...	0.883*	0.943*
Software D	$y = 1.135x - 0.034$	$y = 1.175x - 0.051$	$y = 0.981x + 0.138$	$y = 0.949x + 0.048$	$y = 1.199x - 0.062$	...	0.943*
Software E	$y = 0.907x + 0.043$	$y = 0.942x + 0.027$	$y = 0.797x + 0.195$	$y = 0.773x + 0.103$	$y = 1.069x - 0.056$	$y = 0.754x + 0.099$	...

\* P < .01.

<sup>†</sup> P < .05.

CBV can be calculated by means of several methods, such as the ratio of the area under the time-concentration curve between the tissue and venous output function, and the central volume theorem (CBF × MTT); also, the methods may be different among software. However, in contrast to CBF and MTT, the differences in abnormal area for CBVs and rCBVs among software were small and good correlations were observed between all combinations. These results suggest that CBV and its changes are stable regardless of the algorithms and are comparable between different software.

The quantitative nature of CT perfusion imaging is one of its advantages over MR perfusion imaging, mainly because of the linear relationship between the concentration of contrast material and attenuation number. However, our

results with identical patient data revealed that there were significant differences in the areas with CBF/MTT abnormalities and in rCBF/rMTT values among all software, suggesting that CT perfusion imaging maps obtained with different software can differ in the measurement of perfusion abnormalities because of different sensitivities toward tracer delay. These variations in the quantitative/qualitative results are undesirable and possibly even harmful in certain clinical situations and in multicenter trials. Although previous studies have indicated that the quantitative values obtained with CT perfusion imaging can predict the final infarct size, clinical outcome of the patients, and risk of symptomatic hemorrhage after thrombolysis (2,3,27), these results cannot be generalized before validating intervendor agreement.

To reduce intervendor differences, standardization of scanning protocols, procedures of contrast agent administration, data processing, and data interpretation are needed (28). Susceptibility to the tracer-delay effect is one of most important issues in postprocessing. Steps for refinement of software, including implementation of delay-insensitive algorithms, appear to be necessary, and further cross validation is necessary.

There were several limitations to our study. First, CT perfusion imaging data from only 10 patients were used. Tracer-delay effect was expected to be larger in patients with extracranial hemodynamic compromise, but only one such patient was included in our study group. Further validation should be conducted by using more data sets. Second, we performed subjective delineation

of perfusion abnormalities. If an objective threshold level is used, the results might be different, although the threshold level for each algorithm will be different. In addition, ROIs were obtained by a single operator at a time and interoperator variance was not tested. However, the aim of our study was to analyze the variability among software, and intraoperator agreement was sufficiently high enough to achieve good reproducibility of ROI measurements. Third, we expected the bSVD algorithm, because of its ability to cope with tracer delay, would produce more accurate results than the sSVD algorithm. Additionally, the amount of tracer delay might be estimated by using bSVD, and it might be inversely correlated with CBF or MTT of sSVD. Because these assumptions were not directly validated in this study, further studies should be performed by comparing the results of bSVD with another reference standard for infarction, such as PET or SPECT. Additionally, an adaptive SVD threshold level, such as an oscillation index, was not used with PMA. Wu et al (20) reported better results in their SVD program with an oscillation index. The perfusion maps may differ when using an oscillation index; however, we could successfully classify the software in two groups, the delay-sensitive and delay-insensitive groups, by using the results of the sSVD and bSVD algorithms in PMA. Fourth, the latest version of the software was used when the CT perfusion imaging maps were created; however, the versions tested were not the most current available when this article is published. The newer versions can deal with tracer delay and these versions need to be thoroughly evaluated by using simpler data sets, such as tracer-delay phantom (13).

In conclusion, the abnormal area and relative values of CT perfusion imaging were significantly different among commercially available software provided by CT manufacturers. In particular, overestimation of abnormalities in CBF and MTT, presumably owing to the tracer-delay effect, occurred in software utilizing delay-sensitive algorithms. These variations among soft-

ware should be minimized to improve the reliability of CT perfusion imaging analyses.

**Acknowledgments:** The authors thank T. Itoh (Siemens-Asahi Medical Technologies, Tokyo, Japan), S. Kuwahara (Philips Medical Systems, Tokyo, Japan), M. Okumura (Toshiba Medical Systems, Otawara, Japan), Y. Omi (Hitachi Medical Systems, Kashiwa, Japan), and K. Segawa (GE Healthcare, Tokyo, Japan) for their help in perfusion data analysis and export.

## References

1. Klotz E, Konig M. Perfusion measurements of the brain: using dynamic CT for the quantitative assessment of cerebral ischemia in acute stroke. *Eur J Radiol* 1999;30:170-184.
2. Mayer TE, Hamann GF, Baranczyk J, et al. Dynamic CT perfusion imaging of acute stroke. *AJNR Am J Neuroradiol* 2000;21:1441-1449.
3. Lev MH, Segal AZ, Farkas J, et al. Utility of perfusion-weighted CT imaging in acute middle cerebral artery stroke treated with intra-arterial thrombolysis: prediction of final infarct volume and clinical outcome. *Stroke* 2001;32:2021-2028.
4. Jain R, Hoeffner EG, Deveikis JP, Harrigan MR, Thompson BG, Mukherji SK. Carotid perfusion CT with balloon occlusion and acetazolamide challenge test: feasibility. *Radiology* 2004;231:906-913.
5. Laslo AM, Eastwood JD, Chen FX, Lee TY. Dynamic CT perfusion imaging in subarachnoid hemorrhage-related vasospasm. *AJNR Am J Neuroradiol* 2006;27:624-631.
6. Cenic A, Nabavi DG, Craen RA, Gelb AW, Lee TYA. CT method to measure hemodynamics in brain tumors: validation and application of cerebral blood flow maps. *AJNR Am J Neuroradiol* 2000;21:462-470.
7. Wintermark M, Maeder P, Verdun FR, et al. Using 80 kVp versus 120 kVp in perfusion CT measurement of regional cerebral blood flow. *AJNR Am J Neuroradiol* 2000;21:1881-1884.
8. Hirata M, Sugawara Y, Fukutomi Y, et al. Measurement of radiation dose in cerebral CT perfusion study. *Radiat Med* 2005;23:97-103.
9. Wintermark M, Smith WS, Ko NU, Quist M, Schnyder P, Dillon WP. Dynamic perfusion CT: optimizing the temporal resolution and contrast volume for calculation of perfusion CT parameters in stroke patients. *AJNR Am J Neuroradiol* 2004;25:720-729.
10. Sanelli PC, Lev MH, Eastwood JD, Gonzalez RG, Lee TY. The effect of varying user-selected input parameters on quantitative values in CT perfusion maps. *Acad Radiol* 2004;11:1085-1092.
11. Fiorella D, Heiserman J, Prenger E, Par-tovi S. Assessment of the reproducibility of postprocessing dynamic CT perfusion data. *AJNR Am J Neuroradiol* 2004;25:97-107.
12. Sasaki M, Kudo K, Ogasawara K, Fujiwara S. Tracer delay-insensitive algorithm can improve reliability of CT perfusion imaging for cerebrovascular steno-occlusive disease: comparison with quantitative single-photon emission CT. *AJNR Am J Neuroradiol* 2009;30:188-193.
13. Kudo K, Sasaki M, Ogasawara K, Terae S, Ehara S, Shirato H. Difference in tracer delay-induced effect among deconvolution algorithms in CT perfusion analysis: quantitative evaluation with digital phantoms. *Radiology* 2009;251:241-249.
14. Murphy BD, Fox AJ, Lee DH, et al. White matter thresholds for ischemic penumbra and infarct core in patients with acute stroke: CT perfusion study. *Radiology* 2008;247:818-825.
15. Omi Y, Miyazaki O, Yasuda S, Matsumura A. Development of advanced CT-perfusion software. In: Radiological Society of North America scientific assembly and annual meeting program. Oak Brook, Ill: Radiological Society of North America, 2003.
16. Nambu K, Takehara R, Terada T. A method of regional cerebral blood perfusion measurement using dynamic CT with an iodinated contrast medium. *Acta Neurol Scand Suppl* 1996;93:28-31.
17. Kudo K. Perfusion Mismatch Analyzer, version 3.0.0.0. ASIST-Japan web site. <http://assist.umin.jp/index-e.htm> Published November 2006. Updated February 2009. Accessed February 20, 2009.
18. ASIST-Japan Web site. <http://assist.umin.jp/index-e.htm> Published June 2005. Updated March 2009. Accessed June 9, 2009.
19. Ostergaard L, Weisskoff RM, Chesler DA, Gyldensted C, Rosen BR. High resolution measurement of cerebral blood flow using intravascular tracer bolus passages. Part I. Mathematical approach and statistical analysis. *Magn Reson Med* 1996;36:715-725.
20. Wu O, Ostergaard L, Weisskoff RM, Benner T, Rosen BR, Sorensen AG. Tracer arrival timing-insensitive technique for estimating flow in MR perfusion-weighted imaging using singular value decomposition with a block-circulant deconvolution matrix. *Magn Reson Med* 2003;50:164-174.
21. Calamante F, Gadian DG, Connelly A. Delay and dispersion effects in dynamic

- susceptibility contrast MRI: simulations using singular value decomposition. *Magn Reson Med* 2000;44:466–473.
22. Kudo K, Terae S, Katoh C, et al. Quantitative cerebral blood flow measurement with dynamic perfusion CT using the vascular-pixel elimination method: comparison with H<sub>2</sub>(15)O positron emission tomography. *AJNR Am J Neuroradiol* 2003;24:419–426.
23. Rose SE, Janke AL, Griffin M, Finnigan S, Chalk JB. Improved prediction of final infarct volume using bolus delay-corrected perfusion-weighted MRI: implications for the ischemic penumbra. *Stroke* 2004;35:2466–2471.
24. Silvennoinen HM, Hamberg LM, Lindsberg PJ, Valanne L, Hunter GJ. CT perfusion identifies increased salvage of tissue in patients receiving intravenous recombinant tissue plasminogen activator within 3 hours of stroke onset. *AJNR Am J Neuroradiol* 2008;29:1118–1123.
25. Kucinski T, Naumann D, Knab R, et al. Tissue at risk is overestimated in perfusion-weighted imaging: MR imaging in acute stroke patients without vessel recanalization. *AJNR Am J Neuroradiol* 2005;26:815–819.
26. Matsushima S, Kubota T, Yamada K, et al. Effect of vascular stenosis on perfusion-weighted imaging: differences between calculation algorithms. *J Magn Reson Imaging* 2008;27:1103–1108.
27. Firlik AD, Yonas H, Kaufmann AM, et al. Relationship between cerebral blood flow and the development of swelling and life-threatening herniation in acute ischemic stroke. *J Neurosurg* 1998;89:243–249.
28. Wintermark M, Albers GW, Alexandrov AV, et al. Acute stroke imaging research roadmap. *Stroke* 2008;39:1621–1628.